



AFRL-RX-WP-TP-2011-4298

**REVIEW: MICROSTRUCTURE ENGINEERING OF TITANIUM
ALLOYS VIA SMALL BORON ADDITIONS (Preprint)**

D.B. Miracle

**Metals Branch
Metals, Ceramics, and NDE Division**

S. Tamirisakandala

FMW Composite Systems, Inc.

JULY 2011

Approved for public release; distribution unlimited.

See additional restrictions described on inside pages

STINFO COPY

**AIR FORCE RESEARCH LABORATORY
MATERIALS AND MANUFACTURING DIRECTORATE
WRIGHT-PATTERSON AIR FORCE BASE, OH 45433-7750
AIR FORCE MATERIEL COMMAND
UNITED STATES AIR FORCE**

REPORT DOCUMENTATION PAGE					Form Approved OMB No. 0704-0188	
<p>The public reporting burden for this collection of information is estimated to average 1 hour per response, including the time for reviewing instructions, existing data sources, gathering and maintaining the data needed, and completing and reviewing the collection of information. Send comments regarding this burden estimate or any other aspect of this collection of information, including suggestions for reducing this burden, to Department of Defense, Washington Headquarters Services, Directorate for Information Operations and Reports (0704-0188), 1215 Jefferson Davis Highway, Suite 1204, Arlington, VA 22202-4302. Respondents should be aware that notwithstanding any other provision of law, no person shall be subject to any penalty for failing to comply with a collection of information if it does not display a currently valid OMB control number. PLEASE DO NOT RETURN YOUR FORM TO THE ABOVE ADDRESS.</p>						
1. REPORT DATE (DD-MM-YY) July 2011		2. REPORT TYPE Journal Article Preprint		3. DATES COVERED (From - To) 01 July 2011 – 01 July 2011		
4. TITLE AND SUBTITLE REVIEW: MICROSTRUCTURE ENGINEERING OF TITANIUM ALLOYS VIA SMALL BORON ADDITIONS (Preprint)				5a. CONTRACT NUMBER In-House		
				5b. GRANT NUMBER		
				5c. PROGRAM ELEMENT NUMBER 62102F		
6. AUTHOR(S) D.B. Miracle (Metals, Ceramics, and NDE Division, Metals Branch (AFRL/RXLM)) S. Tamirisakandala (FMW Composite Systems, Inc.)				5d. PROJECT NUMBER 4347		
				5e. TASK NUMBER 20		
				5f. WORK UNIT NUMBER LM10512P		
7. PERFORMING ORGANIZATION NAME(S) AND ADDRESS(ES) Metals, Ceramics, and NDE Division, Metals Branch (AFRL/RXLM) Materials and Manufacturing Directorate Air Force Research Laboratory Wright-Patterson Air Force Base, OH 45433-7750 Air Force Materiel Command, United States Air Force				8. PERFORMING ORGANIZATION REPORT NUMBER AFRL-RX-WP-TP-2011-4298		
9. SPONSORING/MONITORING AGENCY NAME(S) AND ADDRESS(ES) Air Force Research Laboratory Materials and Manufacturing Directorate Wright-Patterson Air Force Base, OH 45433-7750 Air Force Materiel Command United States Air Force				10. SPONSORING/MONITORING AGENCY ACRONYM(S) AFRL/RXLM		
				11. SPONSORING/MONITORING AGENCY REPORT NUMBER(S) AFRL-RX-WP-TP-2011-4298		
12. DISTRIBUTION/AVAILABILITY STATEMENT Approved for public release; distribution unlimited.						
13. SUPPLEMENTARY NOTES PAO case number 88ABW-2010-6058, cleared 15 November 2010. The U.S. Government is joint author of this work and has the right to use, modify, reproduce, release, perform, display, or disclose the work. Submitted to the International Journal of Adv. in Eng. and Applied Mathematics.						
14. ABSTRACT Several studies, dating back to 1950s, were conducted on the addition of boron to titanium alloys, with an aim to improve the stiffness and strength. The majority of these efforts did not lead to successful transition due to shortfalls in mechanical property combinations and insufficient understanding of the effect of boron addition on processing-microstructure-property relationships. Recently, a team of researchers from the US Air Force Research Laboratory critically evaluated boron-modified titanium alloys to assess their applicability for aerospace applications. Several unique opportunities offered by boron-modified Ti alloys were discovered during these evaluations. Boron is essentially insoluble in titanium and precipitates as fine TiB whiskers. Small additions (~0.1 wt.%) of boron to titanium alloys were found to result in dramatically finer grain sizes in the as-cast condition. The presence of TiB precipitates restricts the grain growth at elevated temperatures, even above the beta transus. Together, these features offer the potential to develop affordable thermo-mechanical processing paths for titanium alloys.						
15. SUBJECT TERMS titanium alloys, boron, boron-modified titanium alloys, TiB precipitates						
16. SECURITY CLASSIFICATION OF:			17. LIMITATION OF ABSTRACT: SAR	18. NUMBER OF PAGES 42	19a. NAME OF RESPONSIBLE PERSON (Monitor) Jonathan Spowart	
a. REPORT Unclassified	b. ABSTRACT Unclassified	c. THIS PAGE Unclassified			19b. TELEPHONE NUMBER (Include Area Code) N/A	

Review: Microstructure Engineering of Titanium Alloys via Small Boron Additions

S. Tamirisakandala^{1,2} and D.B. Miracle¹

¹US Air Force Research Laboratory, Materials and Manufacturing Directorate,
Wright-Patterson AFB, OH 45433, USA

²FMW Composite Systems, Inc., Bridgeport, WV 26330, USA

ABSTRACT

Several studies, dating back to 1950s, were conducted on the addition of boron to titanium alloys, with an aim to improve the stiffness and strength. The majority of these efforts did not lead to successful transition due to shortfalls in mechanical property combinations and insufficient understanding of the effect of boron addition on processing-microstructure-property relationships. Recently, a team of researchers from the US Air Force Research Laboratory critically evaluated boron-modified titanium alloys to assess their applicability for aerospace applications. Several unique opportunities offered by boron-modified Ti alloys were discovered during these evaluations. Boron is essentially insoluble in titanium and precipitates as fine TiB whiskers. Small additions (~0.1 wt.%) of boron to titanium alloys were found to result in dramatically finer grain sizes in the as-cast condition. The presence of TiB precipitates restricts the grain growth at elevated temperatures, even above the beta transus. Together, these features offer the potential to develop affordable thermo-mechanical processing paths for titanium alloys. This recent work also demonstrated that, via small boron additions, the strength and stiffness of conventional titanium alloys could be increased up to 20% while retaining acceptable fracture and fatigue properties. In this paper, we review this new class of titanium alloys and describe unique benefits obtained via microstructure engineering.

1. INTRODUCTION

Titanium is the fourth most abundant structural metal in the earth's crust. Accelerating usage of titanium (Ti) alloys is attributable to attractive combinations of low density, high strength, toughness, and corrosion resistance, which render them attractive for a range of applications across the transportation, energy, and consumer goods sectors. Increased strength-to-weight ratio is the primary incentive for selection and design of aerospace applications including engine and airframe components. The use of titanium has been typically limited to aerospace and specialty markets in other sectors. The primary reason for the limited use of titanium alloys is their high cost, about 60% of which, as shown in [Figure 1](#), is associated with energy-intensive melting and fabrication processes for producing titanium products from raw material [\[1\]](#). Thus, there exists a critical need to develop and transition approaches that will improve processibility of titanium alloys thereby decreasing cost and increasing use. Small boron additions to Ti alloys have been found to provide significant benefits in terms of processibility and performance, both of which lead to dramatic improvements in affordability. In this paper, we review this new class of titanium alloys and describe unique benefits obtained via microstructure engineering.

2. HISTORY of Ti-B RESEARCH AND DEVELOPMENT

Early studies conducted at Armor Research Foundation [\[2\]](#) and Royal Aircraft Establishment [\[3\]](#) with an objective to improve the stiffness of titanium concluded that boron is the most effective element to achieve this objective. The increase in Young's modulus by adding 0.5%B was equal to that of 6.5% Al addition.

Using solid-state cold and hot isostatic pressing (CHIP) of blended elemental powders, Dynamet technology has led the development of a family of discontinuously reinforced (TiB and/or TiC) titanium metal matrix composite (CermeTi®) near-net shape products in early 1990s [\[4\]](#). These composites exhibit good room- and elevated-temperature properties and wear resistance. Commercial products such as sporting goods (hockey skate blade, knife blade), tooling for the die-casting industry, military tank-track components, automotive valves and connecting rods, and orthopedic implants were successfully made out of CermeTi® and improvements in performance were demonstrated [\[5\]](#).

Research effort conducted at Boeing under the NASA sponsored High Speed Civil Transportation program [\[6\]](#) considered boron modified titanium alloys to meet improved structural efficiency goals. Approaches included material iteration, process development and mechanical properties characterization. Feasibility of large cast and extruded parts was established. Subscale and full-scale extrusions were made and characterized. This effort showed promise but was discontinued prematurely due to lack of funding, leaving the material with good strength and stiffness but marginal ductility and fatigue properties.

Research conducted in early 1990s at Toyota Motor Corporation [7] on the development of low-cost TiB reinforced titanium matrix composites via a blended elemental powder metallurgy method led to the transition of intake and exhaust valves for the Altezza engine [8]. The valves achieved sufficient durability and reliability with a manufacturing cost acceptable for the mass-produced automobile and motorcycle engine components. More than 500,000 P/M Ti-MMC valves have been put into the market since 1998.

Research work was performed at Crucible Research in early 1990s [9] on the development of discontinuously reinforced titanium alloys via gas atomization of Ti-6Al-4V with additions of boron and/or carbon to make a pre-alloyed in-situ reinforced titanium-alloy powder. The rapid cooling that takes place during atomization resulted in a fine and uniform dispersion of titanium carbide and titanium boride. The atomized powder was consolidated using standard titanium powder consolidation methods such as hot isostatic pressing or extrusion and further processed to produce standard mill forms. Mechanical properties of the consolidated product exhibited room temperature tensile strengths up to 1,470 MPa with an elastic modulus of approximately 140 GPa [10].

Zhu et al. [11] considered addition of a small amount (<0.5%) of boron to cast Ti alloys with the motivation of enhancing mechanical properties for dental applications. They observed significant grain refinement which was attributed to the precipitation of TiB particles. The alloys studied by Zhu et al. were cast in the form of very small size ($45 \times 20 \times 12 \text{ mm}^3$) button ingots using a dental casting machine, and significant oxygen contamination was reported, which could play an important role on the solidification characteristics. While this earlier work provided the first important observation of grain refinement of cast Ti alloys by small boron additions, a number of important details such as quantified assessment and conclusive understanding of the boron effect were not adequately addressed.

Addition of a small amount of boron to γ titanium aluminides (TiAl) has been found to improve room temperature ductility [12]. The principal effect of boron additions γ alloys is to form small TiB₂ particles that refine the lamellar colony size.

3. BASICS of Ti-B MATERIAL SYSTEM

Compositions: Boron is completely soluble in the liquid phase of Ti but is essentially insoluble in the solid Ti phases (high temperature β or room temperature α). Negligible solid solubility of B in Ti eliminates the embrittlement problem commonly caused by other interstitial elements such as H, C, or O. The Ti-rich end of the binary Ti-B phase diagram [13] is shown in Figure 2. The B added to Ti precipitates in the form of intermetallic TiB phase for additions below 18.4 wt.% (50 at.%). TiB formation occurs via an eutectic reaction $\beta + \text{TiB}$ with the binary eutectic composition of ~2 wt.% B. The TiB phase offers several unique advantages. The density of TiB is

comparable to that of Ti but much stiffer and stronger than Ti [14]. Therefore, the TiB phase provides significant increases in stiffness and strength of Ti alloys without density increase providing significant specific weight saving benefit compared to the baseline alloy. The crystal structure of TiB is orthorhombic and particles grow as short whiskers which are efficient strengtheners. TiB has good crystallographic compatibility with Ti providing atomically sharp interfaces. TiB also possesses excellent chemical compatibility as this is the most stable boride phase in Ti-B system. The coefficient of thermal expansion of TiB is comparable to Ti, which eliminates residual stresses at the interfaces. Ti-B materials can be considered as boron-modified Ti alloys at B levels below the eutectic limit (1.55 wt.%B for the most widely used Ti alloy Ti-6Al-4V [15]) since the microstructures, processing, and property combinations are similar to alloys without boron. Above the eutectic limit, the TiB phase is in equilibrium with liquid and rapid growth occurs leading to the formation of coarse primary TiB particles as shown in Figure 3(a) and 3(b) [16]. Although, higher volume fraction of TiB significantly increases stiffness, strength, and wear resistance, the fracture behavior changes from ductile to brittle with increase in B level, causes premature failures (Figure 3c), and results in significant debits in damage tolerance. The microstructures and properties of hypereutectic Ti-B compositions are best classified as discontinuously reinforced titanium metal-matrix composites. A value of 7% minimum tensile elongation is often considered by structural designers for fracture-critical applications. Therefore, Ti-B alloys with low-to-modest B concentrations (<1 wt.%) are relevant to aerospace applications and we focus on these alloys in this paper.

Processing: Ti-B alloys can be produced using traditional processing techniques including liquid metallurgy and powder metallurgy. Various Ti-B alloy processing routes and product forms are illustrated in Figure 4. In the conventional cast metallurgy approach, a boron source (TiB_2 , elemental B, AlB_{12} , or a boron-containing master alloy) is added to Ti alloy charge mix, which completely dissolves and forms a Ti-B alloy melt. Additional Ti is added to compensate for the Ti scavenged from the alloy to transform the B source into TiB. The liquid Ti-B melt can be directly poured into a shaped mold using conventional casting techniques (e.g. investment casting) to produce Ti-B alloy casting or into an ingot mold to produce a Ti-B alloy cast ingot. The TiB phase precipitates during solidification via the eutectic reaction in the cast product. The cast ingot can be subjected to any conventional metalworking process such as forging, rolling, or extrusion to produce a wrought product. Alternatively, the Ti-B alloy melt can be subjected to rapid solidification to produce pre-alloyed (PA) Ti-B powder using conventional powder making processes (e.g. inert gas atomization). The TiB phase forms in the solid state, and is uniformly distributed in each powder particle. PA powder can be outgassed (to remove any volatile impurities) and compacted using techniques such as hot isostatic pressing (HIP) commonly used for Ti alloys to produce near-net shape products. PA powder can also be compacted to billet preforms and subjected to conventional thermo-mechanical processing to manufacture

wrought products. Isotropic properties are obtained when TiB whiskers are randomly oriented but intentional alignment of the TiB through processes such as extrusion or rolling can further increase the properties along the direction of the TiB whiskers. The PA powder approach has the advantage of producing finer length-scale microstructural features due to shorter times for growth during rapid solidification. In addition, the PA approach also offers the advantage of producing supersaturated boron due to non-equilibrium cooling conditions. The supersaturated boron can be precipitated in a controlled fashion via subsequent thermal exposure in the solid state to form nanometer-sized TiB precipitates, as shown in [Figure 5](#), that may provide additional strengthening and improve isotropy. Typical microstructures of Ti-64 containing 1%B produced via cast and PA approach are compared in [Figure 6](#). High aspect ratio TiB in cast alloys and fine length scale TiB with bi-modal size distribution in PA powder alloy are seen in these micrographs. Both cast and PA powder approaches, however, are limited to hypoeutectic compositions as coarse primary TiB particles form in hypereutectic compositions.

Ti-B products can also be manufactured using a blended-elemental (BE) powder metallurgy process which is conducted completely in the solid state ([Figure 4](#)). In the BE powder process, powders of Ti alloy and boron source are intermixed using an appropriate blending process (wet/dry). The powder blend is outgassed and consolidated to prepare a compact. The BE powder compact is then subjected to a reaction heat treatment to convert the boron source into TiB. Like the PA powder process, the BE powder process can also be used to produce either near-net shapes via compaction or net shapes via compaction plus metalworking. The BE approach offers the ability to introduce higher amounts of TiB without the recourse to coarse primary TiB issue since processing is conducted completely in the solid state and is well suited for producing Ti-B composites. The BE powder process has been successfully used to produce several demonstration products (e.g. automobile engine valves). However, the BE powder approach results in coarser plate-like morphology TiB and hollow cores in some cases, as shown in [Figure 6](#), due to the high temperatures (typically above 1200°C) and long times (6–8 hours) required for the completion of boron source to TiB conversion reaction. These aspects of TiB would cause debits in mechanical properties.

4. MICROSTRUCTURE ENGINEERING VIA BORON ADDITION

4.1 Grain Refinement via Trace Boron Addition

Solidification is a dominant processing route for metallic materials, and grain refinement is of significant industrial importance. Fine grain size improves many mechanical properties such as strength, ductility, and damage tolerance, and enhances subsequent mechanical working response. Addition of inoculants to many molten metal alloys (e.g. trace B to Al alloys [\[17\]](#)) is the most commonly used commercial practice to achieve grain refinement but no such grain refinement mechanism is used commercially for Ti alloys. A systematic study evaluating the

effect of trace boron addition to Ti alloys on the grain refinement was performed using 70-mm diameter induction skull melted ingots [18, 19] and the results are summarized in Figure 7. Macrographs recorded on transverse sections of Ti-6Al-4V (Ti-64) and Ti-64-0.06B ingots are shown in Figure 7(a) and 7(b), which illustrate the dramatic grain refinement produced by the trace boron addition. The variation of grain size of Ti-64, Ti-6Al-2Sn-4Zr-2Mo (Ti-6242), unalloyed Ti, and Ti-5Al-5V-5Mo-3Cr (Ti-5553) with boron concentration is shown in Figure 7(c). Addition of about 0.1% boron refines the Ti-64 average as-cast grain size from 1700 μm to 200 μm , the Ti-6242S average grain size from 550 μm to 50 μm , unalloyed Ti average grain size from 500 μm to 50 μm , and Ti-5553 average grain size from 300 μm to 50 μm . The grain size vs. boron concentration curves possess a knee in the range 0.06-0.1%B, which indicates that there exists a critical level of boron required for obtaining dramatic grain refinement. Beyond this B level, only a small additional reduction in grain size occurs. Backscattered electron images of Ti-64 containing various boron levels are presented in Figure 8. In general, both the prior β grain size and α - β colony size decrease as the boron level increases. At 0.02% boron, equiaxed TiB particles of 0.1 vol.% are present, which confirms that the solid solubility of boron in Ti-64 is below this level. The TiB adopts a needle morphology and forms a necklace structure at the prior β grain boundaries for 0.1% B additions. The needle morphology is retained at 0.4%B, but the distribution of TiB becomes more uniform. Similar trends are observed for other Ti alloys with increasing boron levels. Coarse prior β grain boundaries are not present in alloys containing 1% B. Trace B addition also reduced the thickness of grain boundary α phase. The grain boundary α is brittle and reduction in thickness will improve the hot workability. Large size ingots of 125-mm diameter were made via plasma single melting to verify the scale up of grain refinement via trace B addition. Figure 9 shows macrographs in longitudinal and transverse directions of Ti-64 and Ti-64-0.1B ingots. Ti-64 ingot exhibits a columnar grain morphology with grains up to 40-mm length and up to 10-mm width. The addition of 0.1% B results in a substantial refinement of the as-cast structure seen in the macrograph, which confirms the grain refinement in large size ingot. Average cast grain size of 200 μm was recorded in these large ingots.

Although phase diagrams for multi-component Ti alloys with boron are yet to be established, the binary Ti-B phase diagram provides a reasonable guide to understanding the solidification sequence and subsequent microstructural development as shown in Figure 10. In hypoeutectic Ti-B alloys, primary β_{Ti} grains nucleate and grow upon cooling between the liquidus and the eutectic temperatures. Below the eutectic temperature, the remaining liquid trapped between the β_{Ti} grains solidifies via the eutectic reaction, forming an irregular eutectic mixture of β_{Ti} + TiB. Cooling below the β transus motivates the $\beta \rightarrow \alpha$ allotropic transformation as in conventional Ti alloys, and the prior β grain boundaries are retained in the microstructures observed at room temperature. Since the TiB forms after the primary β_{Ti} in hypoeutectic

compositions, the TiB particles cannot act as nucleation sites for the formation of β_{Ti} grains and grain refinement via inoculation is not expected to occur. In view of this, an alternate grain refinement mechanism is necessary to explain the experimental observations.

The grain size obtained after solidification is determined by competition between the nucleation and growth rates. Trace boron additions are likely to enhance the nucleation rate by providing additional driving force and/or slowing the growth rate by influencing the liquid/solid interfacial characteristics. Although more fundamental calculations and/or instrumented experiments are necessary to ascertain the exact grain refinement mechanism via trace boron addition, the following possibilities are proposed to explain the experimental results.

The appearance of equiaxed grains throughout the billet cross sections in all of the castings implies that supercooling arising from a change in composition (constitutional) is more important during solidification than thermal undercooling. The solid solubility of boron in elemental titanium has been established to be below 0.02% [20], and the presence of TiB in Ti-64 containing 0.02%B in this study extends this result to titanium alloys (Figure 8). Thus, boron is rejected from the primary β_{Ti} nuclei into the melt, producing solute partitioning into the liquid ahead of the solidification front. This solute enrichment causes a corresponding variation in the liquidus temperature leading to higher constitutional supercooling (CS). As solidification progresses, CS causes instability at the liquid/solid interface and provides an additional driving force for the nucleation of additional fine β_{Ti} grains ahead of the solid/liquid interface.

Once a nucleus is formed, its growth is influenced by kinetics of atom attachment to the interface, capillarity, and diffusion of heat and mass at the interface and away from the interface. The boron rejected at the solid/liquid interface is likely to influence these factors and restrict the growth of existing nuclei. The excess boron rejected from the solid will accumulate in an enriched boundary layer ahead of the interface. At boron concentrations below a critical value (0.06%), the rejected boron ahead of the interface can be dispersed readily into the remaining liquid and significant grain refinement is not achieved.

When a critical amount of boron is present in the melt, a boron-rich layer retards the growth of the nuclei thereby allowing more nuclei to form in the surrounding supercooled melt, leading to a fine grain size. The degree of grain refinement relies on the balance between latent heat production and heat extraction at the solid/liquid interface. The rate of latent heat production is limited by the solute partitioning at the solid/liquid interface and diffusion in the melt. Grain refinement is expected to improve with an increase in boron level due to higher CS but the experimental observations reveal a saturation in the grain size with boron content and absence of coarse prior β grains at 1% B level. In hypoeutectic alloys, the volume fraction of primary β_{Ti} decreases and eutectic β_{Ti} increases with increase in boron concentration towards the eutectic

limit. The eutectic β_{Ti} precipitates at a finer length scale and coarsening rate would be much slower than that of primary β_{Ti} .

4.2 Microstructural Stability due to TiB Presence

The TiB in Ti alloys with trace B addition ($\sim 0.1\text{B}$) forms a necklace structure, which could enhance microstructural stability during subsequent thermal exposure at elevated temperature by restricting the mobility of grain boundaries via Zener pinning as illustrated in [Figure 11](#) for a beta titanium alloy Ti-15Mo-2.6Nb-3Al-0.2Si. In the case of the baseline alloy, grain growth occurred by about an order of magnitude after thermal exposure above the beta transus for 10 hours, whereas the grain size of the alloy containing 0.1B remained unchanged. The grain size was found to be influenced by the TiB size, orientation, and volume fraction, and could be successfully predicted using a modified Zener pinning model [\[21\]](#). Beta grain growth restriction in the presence of TiB for Ti-64 is illustrated in [Figure 12](#). This macrograph compares the structure of a Ti-64-1B powder compact inside a Ti-64 can, both exposed to 1200°C (200°C above the beta transus) in vacuum for 1 hour and furnace cooled. The average grain size of Ti-64-1B remained unchanged after thermal exposure whereas Ti-64 grains grew from 10 μm to 1000 μm .

Upon cooling from the β to $\alpha+\beta$ phase field, phase transformation from β to α occurs by nucleation and growth according to Burger's orientation relationships. The presence of TiB was found to influence the kinetics of β to α phase transformation by providing additional heterogeneous nucleation sites. [Figure 13](#) compares microstructural evolution of Ti-64-1.7B alloy with that of Ti-64, both of them subjected to thermo-mechanical processing above the beta transus at 1100°C and air cooled to room temperature [\[22\]](#). Equiaxed $\alpha+\beta$ morphology, instead of lamellar $\alpha+\beta$, that occurs in Ti-64 after thermal exposure above the beta transus, occurred in Ti-64B alloy. Equiaxed microstructures, which can only be obtained after extensive $\alpha+\beta$ thermo-mechanical processing, possess better ductility and fatigue initiation resistance compared to lamellar microstructures. Therefore, the presence of TiB offers a novel method to produce equiaxed morphologies without recourse to $\alpha+\beta$ hot work.

4.3 Improved Processability

Grain refinement via trace boron addition may provide opportunities to reduce/eliminate thermo-mechanical processing steps necessary to produce high-quality products. For example, [Figure 14](#) illustrates the influence of boron addition on the rolling response of conventional and boron-modified Ti-64. Both alloys were produced by the same casting method and subjected to rolling under identical conditions in the as-cast condition [\[23\]](#). The alloy without boron exhibited poor workability manifested in the form of severe edge and surface cracks that are attributed to coarse grain size. The alloy containing trace boron, on the other hand, could be

successfully cross rolled without any cracks and the rolled product exhibited good surface finish. Similar observations have been made in forging and extrusion processes. Therefore, boron addition offers the advantage of eliminating expensive and time consuming ingot breakdown steps conventionally practiced to improve the workability of cast microstructure. The presence of TiB also restricts grain growth during hot working and facilitates retention of fine-grained microstructures even after processing at high temperatures.

The TiB whiskers were found to possess excellent thermal stability at conventional processing temperatures as shown in [Figure 15 \[24\]](#). The TiB coarsening rate was insignificant even after thermal exposure at 1300°C for 500 hours. The TiB lengthening rate was also slow at or near the beta transus. Much faster TiB lengthening rates were observed above the beta transus, indicating increased diffusion rates along the length direction.

Since boron is insoluble in titanium under equilibrium conditions, its addition is not expected to influence the beta transus. This has been confirmed in conventionally cast alloys as shown in [Figure 16\(a\) \[15\]](#). In the case of pre-alloyed powder metallurgy Ti-B alloys, a small increase in beta transus was recorded ([Figure 16\(b\)](#)) due to boron modification, which was attributed to the presence of supersaturated boron arising from rapid solidification processing [\[22\]](#). Subsequent thermal exposure of these alloys forces supersaturated boron out of the lattice which combines with Ti to form TiB, the equilibrium microstructure evolves, and the beta transus was found to decrease to that of the baseline alloy.

4.4 Improved Mechanical Properties

The requirement for higher structural efficiency (a combination of stiffness and strength normalized by density) provides a significant motivation for the development of improved aerospace materials and processes. Structurally efficient materials provide a direct path for reducing mass via substitutions with thinner and lighter components, thus improving performance and affordability. A number of advanced aerospace missions, such as hypersonic flight and low-cost access to space, require dramatic reductions in flight mass. Materials with higher structural efficiency can provide enabling capabilities in these applications. Small boron addition to Ti alloys result in important improvements in strength and stiffness. Mechanical properties of Ti-B alloys produced via cast, cast plus wrought, and PA powder metallurgy are presented in this section.

In as-cast Ti-64 alloys, room temperature tensile properties for various boron additions are presented in [Figure 17 \[25\]](#). Microstructural observations indicate an order of magnitude reduction in the prior β grain size, d , as well as a significant reduction in the α lath width, λ , with B additions. It was observed that d and λ are correlated. With the refinement in the microstructure, the yield and ultimate tensile strengths, σ_y and σ_u , respectively, increase

whereas the fracture toughness, K_{IC} , decreases. Modeling of quasi-brittle cleavage fracture indicates that the reduction in K_{IC} with increasing B content is due primarily to the reduced λ . Fatigue crack growth measurements show a gradual reduction in the threshold for fatigue crack propagation with $\sigma_y \lambda^{0.5}$ dependence. Thermo-mechanical processing improves mechanical properties of Ti-B alloys as shown in [Table 1](#) for Ti-64-1.55B in various product forms.

Mechanical properties of Ti-B alloys were found to be dependent on process route. Tensile properties of extruded bars produced via cast via cast and PA approaches are presented [Figure 18](#). Compared to Ti-64, addition of 1%B produces 20-30% improvements in modulus and strength with no debit in ductility. Alloy produced via the PA approach gives larger improvements than the cast approach due to refined microstructural features. These property improvements are found to be maintained at elevated temperatures, thus improving temperature capability.

Boron-modified Ti-64 (Ti-64B) alloys, subjected to various standard heat treatments, exhibited differences in microstructural response to heat treatment compared to that of Ti-64 due to variations in constituent phase fractions and the influence of TiB on the beta-to alpha phase transformation kinetics. Tensile yield strength of hypo- and hyper-eutectic Ti-64B in various heat treated conditions is compared with that of Ti-64 in [Figure 19](#) [26]. The tensile elastic modulus of Ti-64B alloys increased nearly linearly with the boron content (or TiB volume fraction) and the increase could be satisfactorily predicted with an isostrain rule of mixtures (ROMs) and the Halpin–Tsai model. The Ti-64-1B possessed a good combination of tensile strength (1200 to 1370 MPa) and ductility (10 to 13 pct), while Ti-64-1.7B exhibited high strength (1300 to 1695 MPa) and modest ductility (2 to 3.5 pct). Coarse primary TiB particles present in Ti-64-1.7B were found to initiate premature failure [27]. Strength modeling revealed that load sharing by the micron-sized TiB whiskers provides the major contribution for the increase in yield strength. The presence of a small amount of supersaturated boron in these rapidly solidified alloys is likely to provide interstitial solid-solution-strengthening contribution.

A theory for tensile behavior of unidirectional-whisker-reinforced materials was applied to Ti–6Al–4V microstructures and deduced the in situ TiB whisker strength to be 8.0 GPa at a critical length of 10 μm with a Weibull modulus $m = 2$ [28]. With these parameters and the model, the attainment of high tensile elongations could be rationalized and some features of the observed whisker damage evolution could be explained. The success of the model provides guidance for future materials design aimed at maintaining high tensile strength and high elongation in this and other similar material systems.

The overall fatigue life of Ti64-B material compared favorably with that of Ti64 as shown in [Figure 20](#) [29]. The mean fatigue life and standard deviation in life increased with decreasing stress level. The variability in fatigue life increased with decreasing stress level. Two orders of

magnitude of variability, similar to that of Ti-64, were observed at the lower stresses. In assessing the overall fatigue performance of Ti64+1B, the worst case scenario was not driven by TiB particles. Non-metallic inclusions were the life limiting mechanisms in the pre-alloyed powder Ti-64B material, especially in two outlier data points with life less than 10^4 cycles. In the majority of stress-life fatigue tests, including the specimens with subsurface inclusions, most of the life in the test was assumed to have been spent initiating and growing a small crack with little influence of the TiB particles. This study indicated that the time dependent properties of fatigue and crack growth for Ti64-B can be at least as good as and probably a little better than baseline Ti64.

The beneficial aspects of the tensile strengthening translated into enhanced creep resistance with increased B content in as-cast alloys [30]. In the as-cast Ti-64-1B, minimum creep strain rates were around an order of magnitude lower than those for the as-cast Ti-64 alloy at the same applied stress and temperature. Greater B contents also increased the creep-rupture times. The enhanced creep resistance was explained to be a consequence of the load-sharing mechanism by the strong and stiff TiB whiskers that precipitate due to B addition. Hot worked Ti-64-B alloys exhibited significantly greater creep resistance than the as-cast alloys due to improved microstructural homogeneity. Among all Ti-64-1B alloys via different processing routes, the PA PM extruded Ti-64-1B alloy exhibited the lowest creep resistance, although its fatigue resistance was the greatest.

5. CONCLUSIONS

- i) Small boron additions to titanium alloys offer opportunities to engineer microstructures that could improve processability and performance.
- ii) Trace boron additions refine cast grain size by an order of magnitude.
- iii) The presence of TiB precipitates restricts the grain growth at elevated temperatures, even above the beta transus.
- iv) Grain refinement and grain stability offer the potential to develop affordable thermo-mechanical processing paths for titanium alloys.
- v) Small boron additions provide 20% increase in strength and modulus relative to the baseline while retaining good fracture-critical properties.
- vi) Control of composition, processing, and thermo-mechanical processing, which influence the microstructure, were identified as key factors in the maturation of Ti-B alloys for fracture-critical applications.

Acknowledgements

This work was conducted as part of in-house research at the Materials and Manufacturing Directorate, Air Force Research Laboratory, Wright-Patterson AFB, OH, USA. The authors acknowledge contributions made by several collaborators.

REFERENCES

1. Gambogi and Gerdemann: "Titanium Metal: Extraction to Application" US DOE Report ARC-1999-060
2. W.H. Graft, D.W. Levinson, W. Rostoker, Trans. ASM, 49 (1957) 263
3. A.R.G. Brown, H. Brooks, K.S. Jepson, G.I. Lewis, Tech. Note No. MET/PHYS 343, Royal Aircraft Establishment, Ministry of Aviation, London, Sep 1961.
4. Abkowitz S., Weihrauch P. F., Heussi H. L. and Abkowitz S., "P/M Titanium Matrix Composites: From War Games to Fun & Games", Titanium '95: Science and Technology, Proceedings of the eighth world conference on Titanium, 22-26 Oct.1995, held at Birmingham, UK, Eds. Blenkinsop P.A. et al., The Institute of Materials, London, 1996), 2722-2730.
5. S. Abkowitz, S.M. Abkowitz, H. Fisher, P.J. Schwartz, JOM, 56:5 (2004) 37-41.
6. High speed research – Airframe technology, MDC Report CRAD-9408-TR-2679, Jan 1997.
7. Saito T., Furuta T. and Yamaguchi T., "Development of Low Cost Titanium Matrix Composite", Recent Advances in Titanium Metal Matrix Composites, (Proceedings of a symposium held during Materials Week, October 2-6, 1994, Rosemont, Illinois, Eds.Froes F.H. and Storer J., The Minerals, Metals & Materials Society, 1995), 33-44.
8. T. Saito, JOM, 56:5 (2004) 33-36.
9. Yolton C.F. and Moll J.H., "Evaluation of a Discontinuously Reinforced Ti-6Al-4V Composite" Titanium '95: Science and Technology, (Proceedings of the eighth world conference on Titanium, 22-26 Oct.1995, held at Birmingham, UK, Eds. P.A. Blenkinsop et al., The Institute of Materials, London,1996), 2755-2762.
10. C.F. Yolton, JOM, 56:5 (2004) 56-59.
11. Zhu et al. Mater. Sci. Eng. A 2003; 339:53
12. J.A. Christodoulou and H.M. Flower, Adv. Eng. Mater. 2 (2000) pp. 631-8.
13. Murray, Binary Phase Diagrams ASM Handbook
14. Godfrey: Adv Eng Mater 2000:2, 85
15. O.M. Ivasishin, R.V. Teliovich, V.G. Ivanchenko, S. Tamirisakandala, D.B. Miracle, Metall. Mater. Trans. 39A (2008) 402-416.
16. S. Lieberman, Doctoral dissertation, Georgia Institute of Technology, Atlanta GA, 2007.
17. Greer AL, Cooper PS, Meredith MW, Schneider W, Schumacher P, Spittle JA, et al. Adv Eng Mater 2003;5:81.
18. S. Tamirisakandala, Scripta Mater. 53 (2005) 1421–1426
19. S. Tamirisakandala, J Mater. Eng. Perf. 14 (2005) 741-746.
20. Palty AE, Margolin H, Nielsen JP: Trans. ASM 1954:46:312
21. B. Cherukuri, R. Srinivasan, S. Tamirisakandala, D.B. Miracle: Scripta Mater. 60 (2009) 496-499.

22. S. Tamirisakandala, R.B Bhat, D.B. Miracle, S. Boddapati, R. Bordia, R. Vanover, V.K. Vasudevan, *Scripta Mater.* 53 (2005) 217-222.
23. R. Srinivasan, M.D. Bennett, S. Tamirisakandala, D.B. Miracle, K.O. Yu, F. Sun, *J Mater. Eng. Perf.* 18:4 (2009) 390-398.
24. D.J. McEldowney, PhD Thesis, Univ. Dayton, 2006.
25. I. Sen, S. Tamirisakandala, D.B. Miracle, U. Ramamurty, *Acta Mater.* 55 (2007) 4983-4993.
26. D.J. McEldowney, S. Tamirisakandala, D.B. Miracle, *Metall. Mater. Trans.* 41A (2010) 1003-1015.
27. I. Sen, L. Maheshwari, S. Tamirisakandala, D.B. Miracle, U. Ramamurty, *Mater. Sci. Eng. A* 518 (2009) 162-166.
28. C.J. Boehlert, S. Tamirisakandala, W.A. Curtin, D.B. Miracle, *Scripta Mater.* 61 (2009) 245–248.
29. K. Schwendiman, MS Thesis, AFIT, 2007
30. W. Chen, PhD Thesis, Michigan State University, Lansing MI, 2010.

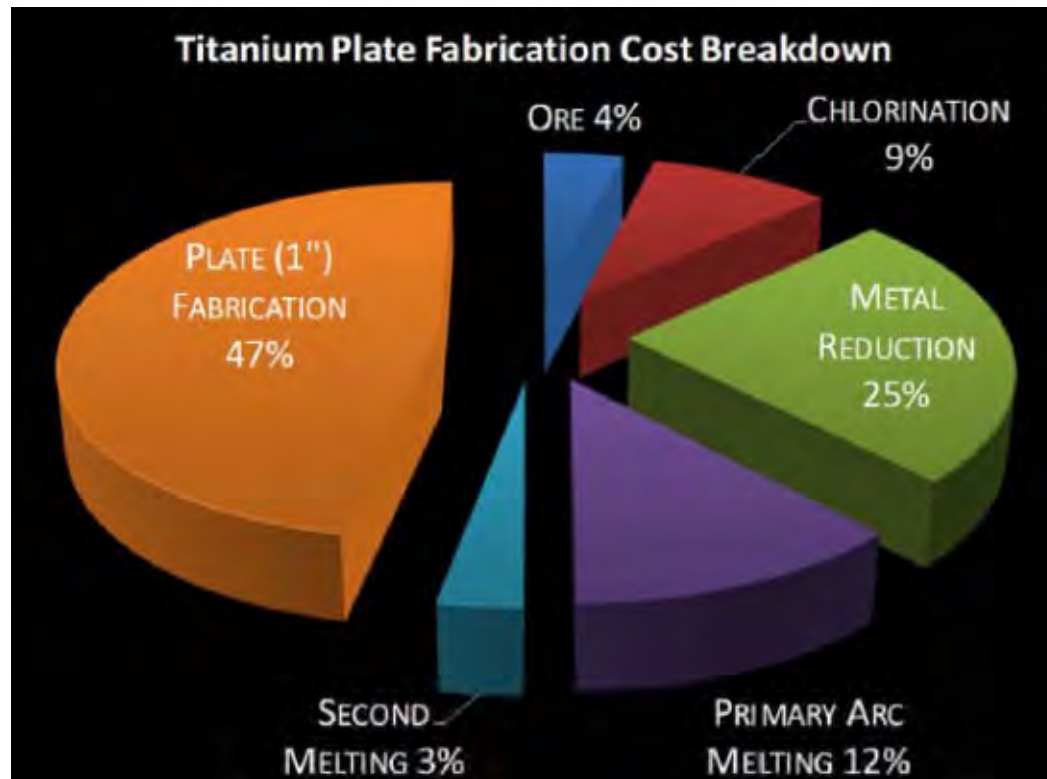
List of Figures

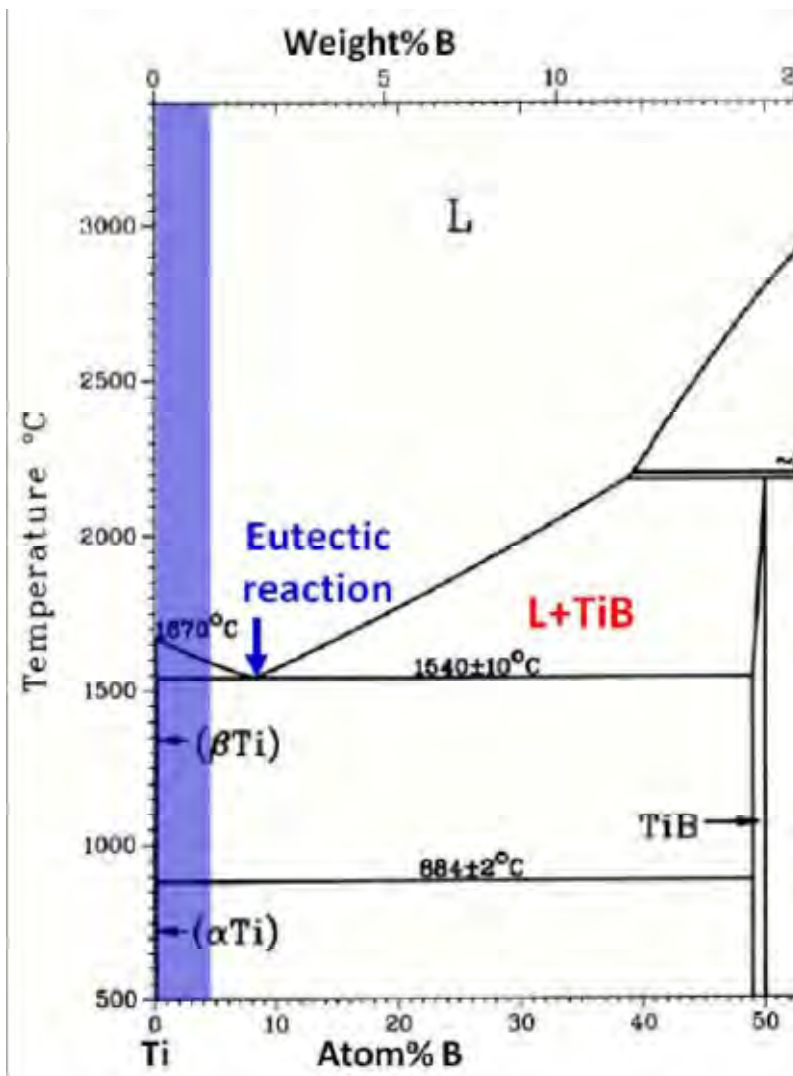
- Figure 1 Break down of titanium plate fabrication cost.
- Figure 2 Ti-B binary phase diagram.
- Figure 3 (a) Micrograph (backscattered electron image) of hypereutectic Ti-64-B alloy (Ti-64-1.7B) showing primary and eutectic TiB, (b) 3D microstructure of individual primary and eutectic TiB, (c) tensile fracture surface of Ti-64-1.7B showing preferential fracture initiation at primary TiB.
- Figure 4 Process routes for producing boron-modified titanium alloys.
- Figure 5 Micrographs (backscattered electron images) of cross-sections of (a) as-atomized powder particle and (b) heat treated powder particle that exhibits fine length scale TiB precipitated from the supersaturated boron.
- Figure 6 Comparison of microstructures of Ti-64-B produced via cast, pre-alloyed powder and blended elemental powder approaches.
- Figure 7 Macrographs of (a) Ti-64 and (b) Ti-64-0.06B ingot cross-sections. (c) variation of average as-cast grain size with boron content for various Ti alloys.
- Figure 8 Backscattered electron images of cast Ti-64 containing boron levels indicated on the micrographs. The gray background is the α , bright phase is the β , and dark phase is the TiB.
- Figure 9 Macrographs of plasma single melt Ti-64 and Ti-64-0.1B ingots showing grain refinement.
- Figure 10 Illustration of grain refinement mechanism in titanium alloys modified with boron.
- Figure 11 Microstructure of Beta 21S and Beta 21S-0.1B in the as-cast condition and after annealing at 960°C for 10 h. Micrographs (a), (b) and (d) are backscattered electron images, and macrograph (c) is a montage of optical photographs with traced grain boundaries. The graph shows variation of β grain size as a function of annealing time at different temperatures for Beta21S and Beta21S-0.1B.
- Figure 12 Macrograph of transverse section of Ti-64-1B powder compact made in Ti-64 can, both subjected to vacuum anneal at 1200°C for 1 hour.
- Figure 13 Micrograph in the transverse direction of Ti-64-1.7B extrusion at the can-billet interface.
- Figure 14 Rolled plates and sheets produced from Ti-64 and Ti-64-0.1B ingots cast by the plasma arc melting (PAM) and induction skull melting (ISM) techniques.
- Figure 15 Thermal stability of TiB as a function of temperature and time.
- Figure 16 (a) Calculated (solid line) and experimentally measured beta transus values of Ti-64 as a function of boron content. (b) beta approach curves established via metallography on water-quenched samples of Ti-64, Ti-64-1B, and Ti-64-1.7B.

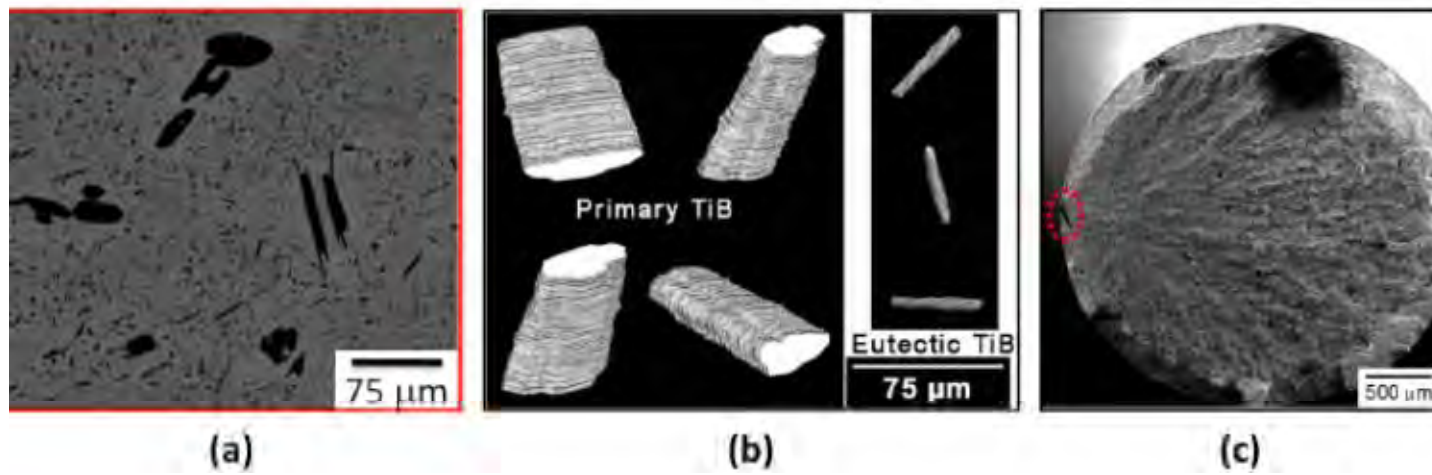
- Figure 17 Variations of tensile yield strength (YS), ultimate tensile strength (UTS), tensile elongation (e), and fracture toughness (K_{Ic}) with boron content in as-cast Ti-64 alloys.
- Figure 18 Room temperature tensile properties of extruded Ti-64-1B alloys produced via cast and pre-alloyed powder metallurgy approaches.
- Figure 19 (a) Tensile yield strength of Ti-64B alloys in various heat treated conditions compared with Ti-64 data (b) tensile elastic modulus of Ti-64-B alloys as a function of TiB volume fraction predicted from the rule of mixtures (ROM) and the Halpin-Tsai model compared with experimental values.
- Figure 20 Fatigue life variability of Ti-64-1B alloy compared with Ti-64.

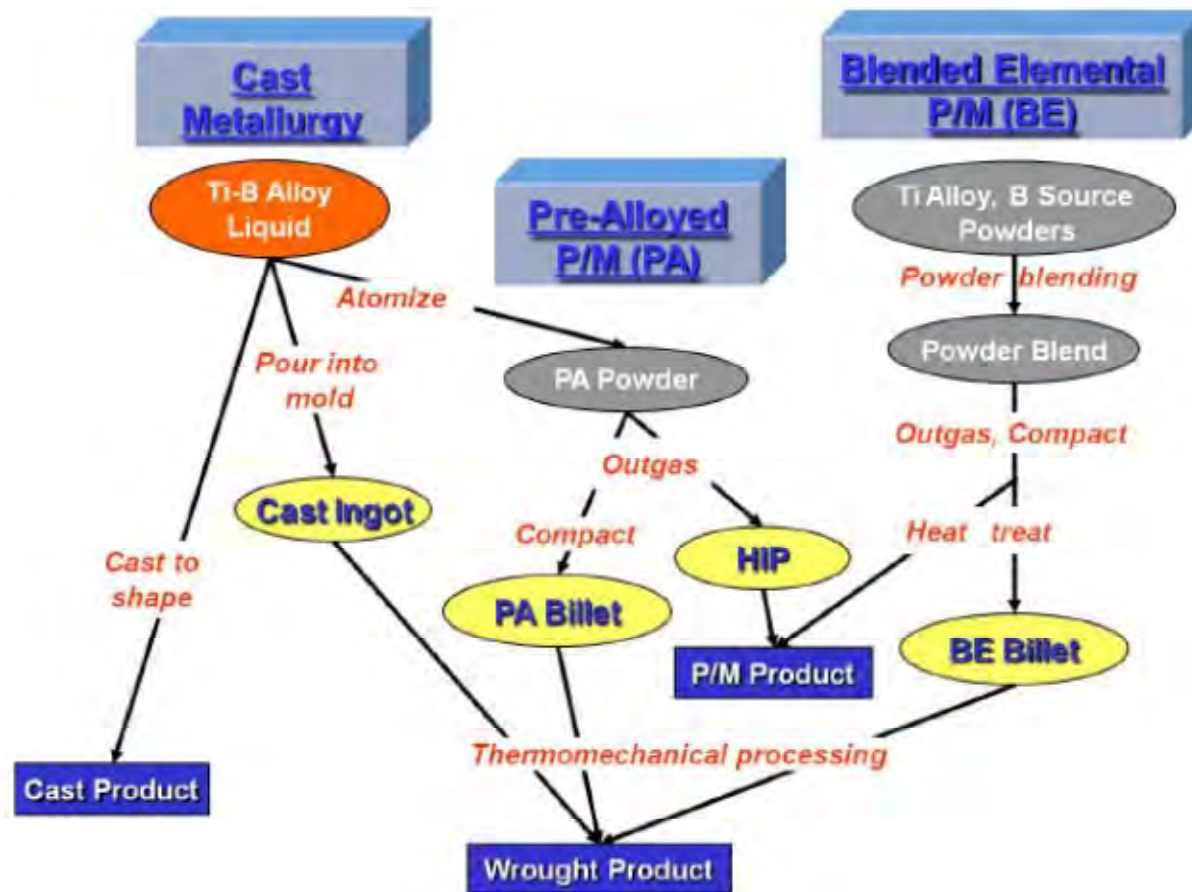
Table 1. Tensile properties of Ti-64-1.55B made via cast approach

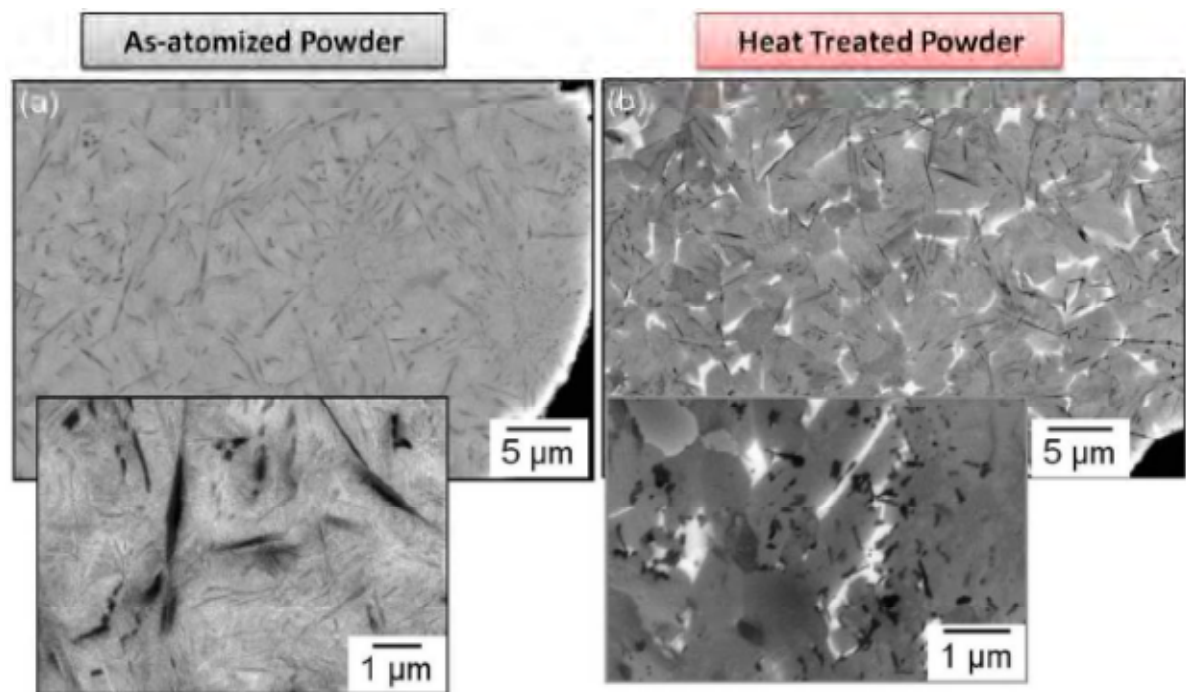
Property	As-Cast	Forged	Rolled	Extruded
YS, MPa	999	1065	1170	1185
UTS, MPa	1033	1128	1230	1200
<i>E</i> , GPa	138	132	142	148
<i>e</i> , %	0.9	2.7	6	5

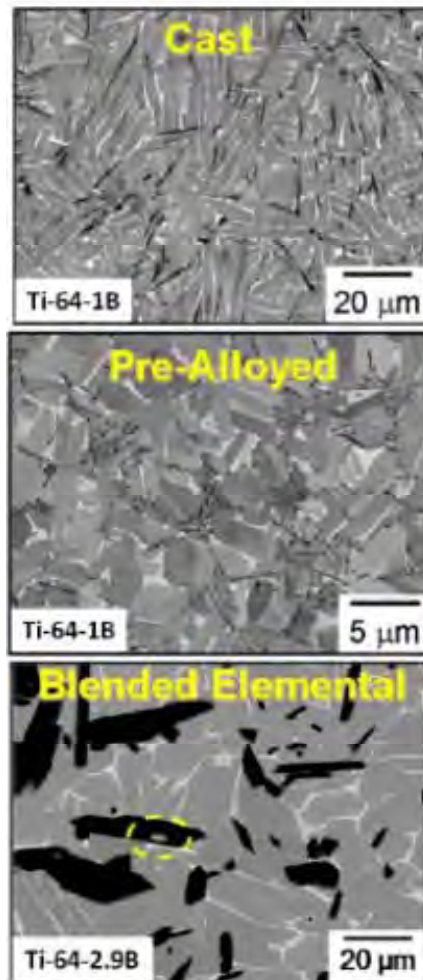


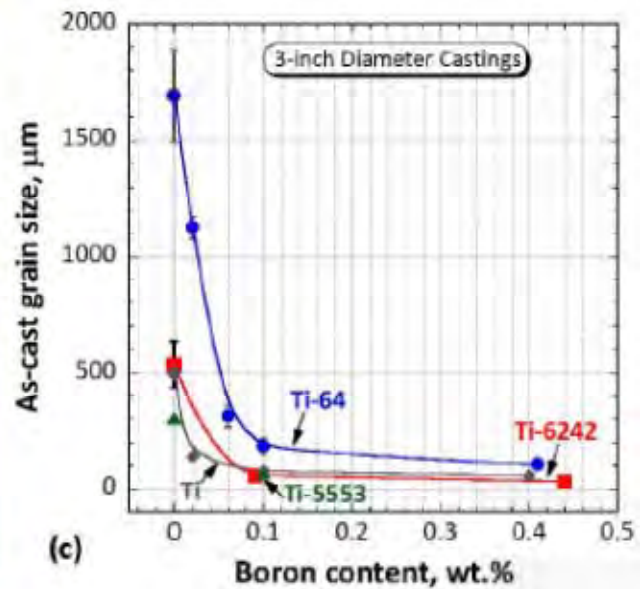
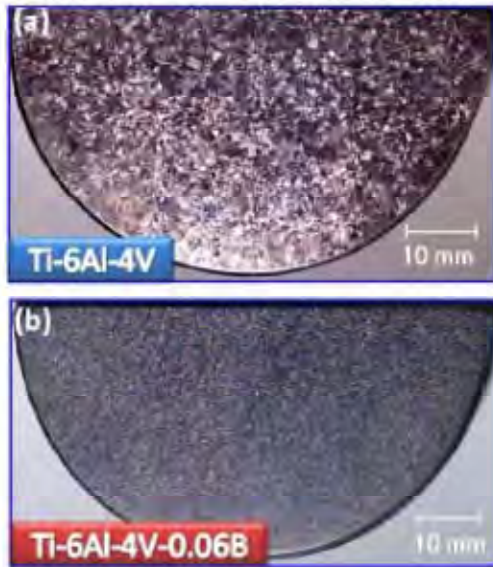


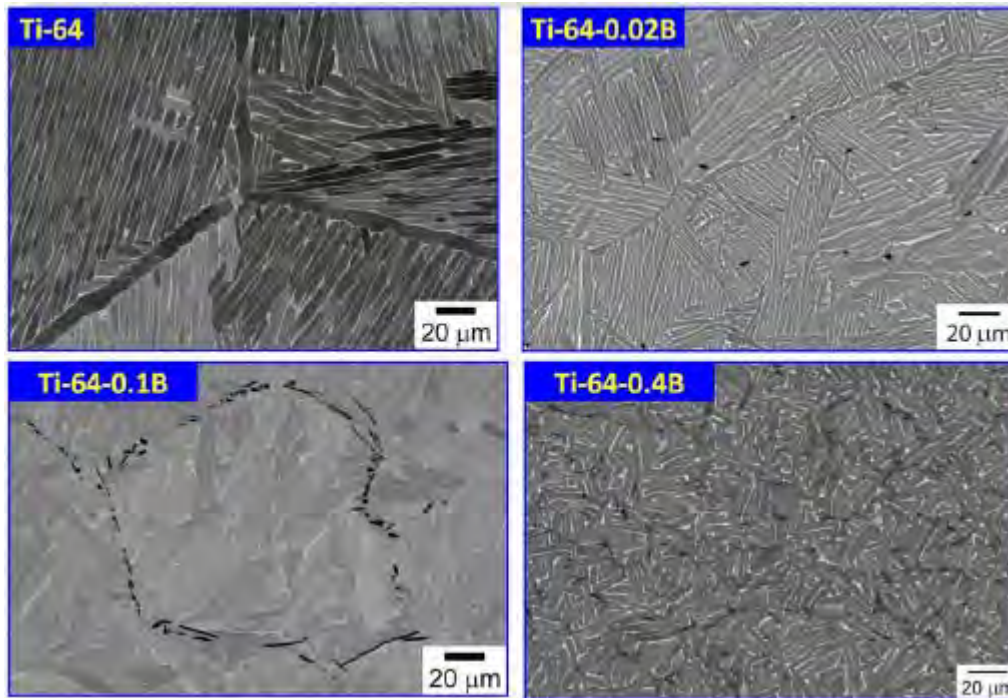


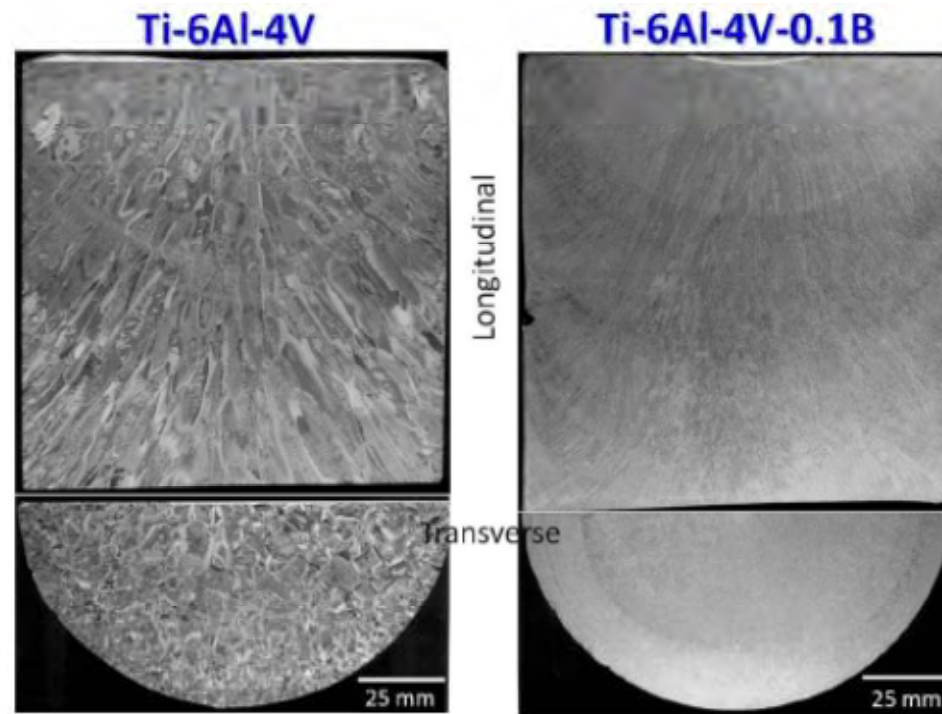


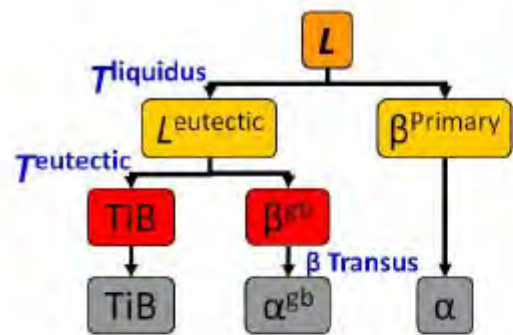








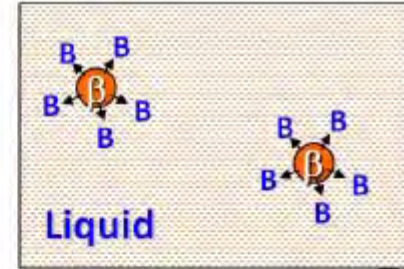




Solidification sequence

$T_{\text{eutectic}} < T < T_{\text{liquidus}}$

$T < \beta_{\text{Transus}}$



$T < T_{\text{liquidus}}$

